

Multi-watt laser operation and laser parameters of Ho-doped Lu₂O₃ at 2.12 μm

Philipp Koopmann,^{1,2,*} Samir Lamrini,² Karsten Scholle,²
Michael Schäfer,² Peter Fuhrberg,² and Günter Huber¹

¹Institute of Laser-Physics, University of Hamburg, Luruper Chaussee 149,
22761 Hamburg, Germany

²LISA laser products, Max-Planck-Str. 1, 27191 Katlenburg-Lindau, Germany

*philipp.koopmann@physnet.uni-hamburg.de

Abstract: We present spectroscopic investigations and the first laser operation of Ho:Lu₂O₃. Laser operation was obtained with two different setups at room temperature: In a 1.9 μm diode pumped setup a maximum output power of 15 W was achieved. With a Tm-fiber laser pumped setup the maximum output power was 5.2 W and the slope efficiency was 54 % with respect to the absorbed pump power. Absorption measurements revealed absorption cross sections of up to $11.7 \cdot 10^{-21} \text{ cm}^2$ at 1928 nm. In the 2.1 μm range a maximum emission cross section of $4.5 \cdot 10^{-21} \text{ cm}^2$ at 2124 nm was determined, which remains the highest gain peak even for high inversions. The fluorescence lifetime of the ⁵I₇-manifold was found to be 10 ms.

© 2011 Optical Society of America

OCIS codes: (140.3070) Infrared and far-infrared lasers; (140.3580) Lasers, solid-state.

References and links

1. K. Scholle, S. Lamrini, P. Koopmann, and P. Fuhrberg, "2 μm Laser Sources and Their Possible Applications," in *Frontiers in Guided Wave Optics and Optoelectronics*, B. Pal, ed. (Intech, Vukovar, Croatia, 2010), pp. 471–500.
2. E. Lippert, S. Nicolas, G. Arisholm, K. Stenersen, and G. Rustad, "Midinfrared laser source with high power and beam quality," *Appl. Opt.* **45**, 3839–3845 (2006).
3. T. Y. Fan, G. Huber, R. L. Byer, and P. Mitzscherlich "Spectroscopy and Diode Laser-Pumped Operation of Tm:Ho:YAG," *IEEE J. Quantum Electron.* **23**, 924–933 (1988).
4. G. Rustad and K. Stenersen, "Modeling of Laser-Pumped Tm and Ho Lasers Accounting for Upconversion and Ground-State Depletion," *IEEE J. Quantum Electron.* **32**, 1645–1656 (1996).
5. D.Y. Shen, A. Abdolvand, L.J. Cooper, and W.A. Clarkson, "Efficient Ho : YAG laser pumped by a cladding pumped tunable Tm : silica-fibre laser," *Appl. Phys. B* **79**, 559–561 (2004).
6. X. Mu, H.E. Meissner, and H.-C. Lee, "Thulium Fiber Laser 4-Pass End-Pumped High Efficiency 2.09-μm Ho:YAG Laser," in "Proceedings of CLEO/QUELS 2009," (2009), CWH1.
7. C.D. Nabors, J. Ochoa, T.Y. Fan, A. Sanchez, H.K. Choi, and G.W. Turner, "Ho : YAG Laser Pumped By 1.9-μm Diode Lasers," *IEEE J. Quantum Electron.* **31**, 1603–1605 (1995).
8. S. Lamrini, P. Koopmann, M. Schäfer, K. Scholle, and P. Fuhrberg, "Efficient High-Power Ho:YAG Laser Directly in-Band Pumped by a GaSb-Based Laser Diode Stack at 1.9 μm," *Appl. Phys. B* (2011). DOI: 10.1007/s00340-011-4670-5
9. R. Peters, C. Kränkel, S. Fredrich-Thornton, K. Beil, K. Petermann, G. Huber, O. Heckl, C. Baer, C. Saraceno, T. Südmeyer, and U. Keller, "Thermal analysis and efficient high power continuous-wave and mode-locked thin disk laser operation of Yb-doped sesquioxides," *Appl. Phys. B* **102**, 509–514 (2011).
10. C. R. E. Baer, C. Kränkel, C. J. Saraceno, O. H. Heckl, M. Golling, R. Peters, K. Petermann, T. Südmeyer, G. Huber, and U. Keller, "Femtosecond thin-disk laser with 141 W of average power," *Opt. Lett.* **35**, 2302–2304 (2010).

11. P. Koopmann, S. Lamrini, K. Scholle, P. Fuhrberg, K. Petermann, and G. Huber, "Efficient diode-pumped laser operation of Tm:Lu₂O₃ around 2 μm," *Opt. Lett.* **36**, 948–950 (2011).
12. L. Fornasiero, E. Mix, V. Peters, K. Petermann, and G. Huber, "Czochralski growth and laser parameters of RE³⁺-doped Y₂O₃ and Sc₂O₃," *Ceram. Int.* **26**, 589–592 (2000).
13. J. Mohr, M. Mond, V. Peters, E. Heumann, K. Petermann, and G. Huber, "Spectroscopy and continuous wave lasing of Yb,Ho:Sc₂O₃ and Tm,Ho:Sc₂O₃ at 2.1mm," DPG-Frühjahrstagung 2001, Q 33.4, available at http://old.dpg-tagungen.de/archive/2001/html/q_33.html (2001).
14. G. A. Newburgh, A. Word-Daniels, A. Michael, L. D. Merkle, A. Ikesue, and M. Dubinskii, "Resonantly diode-pumped Ho³⁺:Y₂O₃ ceramic 2.1 μm laser," *Opt. Express* **19**, 3604–3611 (2011).
15. M. Galceran, M. C. Pujol, P. Gluchowski, W. Streck, J. J. Carvajal, X. Mateos, M. Aguilo, and F. Diaz, "A Promising Lu_{2-x}Ho_xO₃ Laser Nanoceramic: Synthesis and Characterization," *J. Am. Ceram. Soc.* **93**, 3764–3772 (2010).
16. F. Schmid, and D. Viehnicki, "Growth of Sapphire Disks from the Melt by a Gradient Furnace Technique," *J. Am. Ceram. Soc.* **53**, 528–529 (1970).
17. R. Peters, C. Kränkel, K. Petermann, and G. Huber, "Crystal growth by the heat exchanger method, spectroscopic characterization and laser operation of high-purity Yb:Lu₂O₃," *J. Cryst. Growth* **310**, 1934–1938 (2008).
18. M. Fechner, F. Reichert, P. Koopmann, K. Petermann, and G. Huber, "Spectroscopy of Ho:Lu₂O₃ with Respect to the Realization of a Visible Laser," in "Proceedings of CLEO Europe EQEC 2011," (2011), CA8.4.
19. D. E. McCumber, "Einstein Relations Connecting Broadband Emission and Absorption Spectra," *Phys. Rev.* **136**, A954–A957 (1964).
20. V. Peters, "Growth and Spectroscopy of Ytterbium-Doped Sesquioxides," PhD thesis, University of Hamburg (Shaker, 2001).
21. S. A. Payne, L. L. Chase, L. K. Smith, W. L. Kway, W. F. Krupke, "Infrared Cross-Section Measurements for Crystals Doped with Er³⁺, Tm³⁺, and Ho³⁺," *IEEE J. Quantum Electron.* **28**, 2619–2630 (1992).

1. Introduction

Laser systems with wavelengths in the spectral region around 2 μm have a large field of applications in medicine, gas detection, LIDAR systems, and pumping of OPOs for the conversion into the mid-infrared spectral region [1]. The most common approaches for the generation of 2 μm laser radiation are thulium- and holmium-doped solid state lasers. Thulium exhibits the advantage of a cross relaxation process which permits pumping these systems at around 800 nm, where high-performance laser diodes are commercially available, and lasing at 2 μm with a quantum efficiency of up to two. Nevertheless, these systems suffer from larger quantum defects, lower emission cross sections and shorter lifetimes in comparison to holmium-based laser systems. Furthermore, Tm-based laser systems commonly emit in the 1.8 μm to 2.0 μm region where strong water absorption is present, while the wavelengths of holmium-based lasers are in the area of 2.1 μm, where the water absorption is strongly reduced. Additionally the longer wavelengths are beneficial for the excitation of ZGP (zinc germanium phosphide), a nonlinear crystal used for the conversion to the mid-infrared, since the absorption in these crystals decreases with increasing wavelength and thus a higher conversion efficiency can be achieved [2].

The challenge for holmium lasers is the excitation of the Ho³⁺-ions. In the past this has often been achieved by codoping crystals with holmium and thulium and exploiting an efficient energy transfer process from the thulium ions to the holmium ions [3]. These systems can be pumped at around 800 nm, however their efficiency is strongly limited mainly due to upconversion processes [4]. An alternative is the direct excitation of Ho³⁺-ions with 1.9 μm lasers. Commonly thulium lasers are used and utilizing their high beam quality compared to diode lasers, holmium lasers with slope efficiencies of up to 80 % could be realized [5, 6]. Since these systems are complex and bulky, the goal is the realization of compact diode pumped holmium lasers. Recent progress in the development of laser diodes in the 1.9 μm region now gives prospect to efficient high power diode pumped holmium lasers in the near future.

So far only little research has been performed on diode pumped holmium lasers. First approaches were carried out in 1995 by Nabors et al., who utilized GaInAsSb-InGaAsP-based

laser diodes at 1.9 μm to pump a Ho:YAG crystal. They achieved a slope efficiency of 35 % and an output power of 0.7 W at -53°C [7]. Increasing the crystal temperature led to a strong decrease of the output power. Newly developed GaSb-based high power laser diodes enabled a diode pumped Ho:YAG laser with an output power of 55 W and a slope efficiency of 62 % at room temperature [8].

Among research activities targeting efficient pump sources at 1.9 μm also material research of the crystal host has to be performed. In the last years the sesquioxides have proven to have favorable properties for high power lasers, especially when doped with ytterbium and thulium [9, 10, 11]. The main reasons for this are the high thermal conductivities and the high emission cross sections of these materials. Furthermore, the low phonon energies of these hosts lead to reduced non-radiative processes and the strong Stark splitting leads to less reabsorption, which is important for quasi three level lasers. Nevertheless due to the challenging growth of these crystals only few publications on holmium doped sesquioxides exist. Some spectroscopic data on Ho:Sc₂O₃ and Ho:Y₂O₃ are presented in [12].

First evidence of laser operation in holmium-doped sesquioxides can be found in [13], where laser operation was achieved with Ho:Sc₂O₃ codoped with ytterbium and thulium.

Recently first attempts on diode pumping of holmium doped Y₂O₃ ceramics were carried out [14]. Due to the limited quality of the ceramic, laser oscillation could only be achieved at cryogenic temperatures. An output power of 2.5 W and a slope efficiency of 35 % were obtained.

Galceran et al. recently published spectroscopic investigations on holmium doped Lu₂O₃ nano-ceramics and nano-crystals [15]. They conclude, that Ho:Lu₂O₃ is a promising laser material, but so far the ceramic quality was not sufficient for laser experiments.

Due to its long lifetime, its high thermal conductivity even when doped with rare earth ions, and the feasibility of the growth of high quality crystals, holmium-doped Lu₂O₃ was chosen for this work. We grew a 0.3 at.% doped crystal by the Heat-Exchanger Method (HEM) [16, 17]. Absorption and emission spectra were measured, the upper laser level lifetime was determined and for the first time laser oscillation was obtained in this crystal with two different pumping schemes: A diode pumped and a fiber laser pumped setup. At room temperature output powers of up to 15 W (diode pumped) and 5.2 W (fiber laser pumped), respectively, were obtained. In the fiber laser pumped setup the maximum slope efficiency was 54 % with respect to the absorbed pump power.

2. Crystal Growth

Besides many mentioned favorable properties, sesquioxides suffer from one property which makes the crystal growth challenging: A melting temperature of more than 2400 $^\circ\text{C}$ which is $\sim 500^\circ\text{C}$ higher than the melting point of other common oxide laser crystals. Due to the high melting point it has so far not been possible to grow large sesquioxide crystals by the well established Czochralski method. During the last years high quality sesquioxide crystals could be grown by the Heat-Exchanger Method which is in detail described in [17]. For the growth a rhenium crucible is used, which is cooled from the bottom, where the seed crystal is placed. When the whole material except the seed crystal is molten, the cooling is increased and therefore the crystal grows from the bottom into the melt. Since the crystal gets into contact with the crucible walls at a late point of the growth, low-stress boules can be produced.

For assuring a minimized impact of upconversion effects for the laser, a Ho:Lu₂O₃ crystal with a low dopant concentration of 0.3 at.% was grown. As the ionic radii of the Ho³⁺ (0.9 \AA) and the Lu³⁺ (0.86 \AA) ions do not deviate strongly, a distribution coefficient near unity was assumed and could be verified by absorption measurements on crystal samples originating from the bottom and the top of the crystal boule, respectively.

3. Spectroscopy

Absorption Spectrum

The absorption spectrum of the Ho(0.3%):Lu₂O₃ crystal was measured with a Cary 5000 spectrophotometer set to a resolution of 0.5 nm. The highest absorption cross section peaks can be found in the visible spectral region (up to $2.1 \cdot 10^{-19}$ cm² at 448 nm). An insight on utilizing this absorption for the realization of visible lasers is given in [18]. For 2 μm lasers the absorption in the 1.9 μm range shown in Fig. 1a is crucial. An enlarged view of the relevant region of this spectrum is shown in the inset of Fig. 1a and in Fig. 3. Absorption cross sections of up to $11.7 \cdot 10^{-21}$ cm² and $10.2 \cdot 10^{-21}$ cm² can be found at 1928 nm and 1940 nm, respectively. Even though the four peaks between 1926 nm and 1942 nm are relatively narrow (FWHM ~ 3 nm), the absorption cross section is above $3.5 \cdot 10^{-21}$ cm² for the whole region. Since commercially available laser diodes in the 1.9 μm range still exhibit relatively broad emission spectra, a broad absorption spectrum is important for efficiently exciting the crystal.

The peak absorption cross sections are about two times as high as reported by Galceran et al. [15], which can presumably be attributed to a higher resolution of our measurement, as the values in the smooth parts of the spectrum are similar, but a larger number of peaks can be found in Fig. 1a.

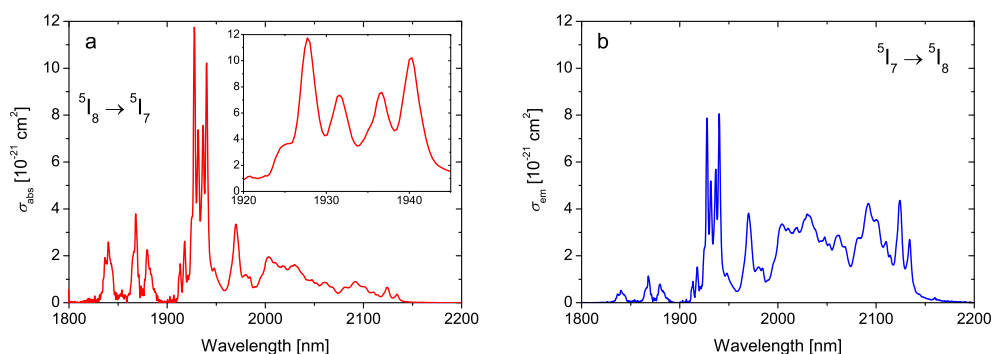


Fig. 1. Room temperature absorption (a) and emission (b) cross section spectra of Ho:Lu₂O₃ around 2 μm. The inset in (a) shows the region from 1920 nm to 1945 nm, where the maximum absorption cross sections are located.

Emission Spectrum

The fluorescence spectrum was recorded with a Bruker Equinox 55 Fourier transform spectrometer. The emission cross section spectrum was then calculated from the absorption spectrum via the McCumber relation [19] and from the fluorescence spectrum using the Füchtbauer-Ladenburg equation. The energy of the Stark levels needed for the McCumber relation was derived from [20]. The emission spectrum shown in Fig. 1b is a combination of the two spectra with the McCumber spectrum covering the short- and the Füchtbauer-Ladenburg spectrum covering the long-wavelength region (> 2000 nm). This way the regions where the two spectra suffer from reabsorption (Füchtbauer-Ladenburg) and noise (McCumber) could be eliminated.

The emission spectrum shows two peaks in the long wavelength region, where free running laser operation can be expected. The peaks are located at 2124 nm and 2134 nm. The respective emission cross sections are $4.5 \cdot 10^{-21}$ cm² and $2.3 \cdot 10^{-21}$ cm².

Gain Spectra

From the absorption and emission spectra the gain spectra were calculated via $\sigma_{\text{gain}} = \beta\sigma_{\text{em}} - (1 - \beta)\sigma_{\text{abs}}$ for different inversion levels $\beta = \frac{N_2}{N_{\text{tot}}}$, where N_2 and N_{tot} are the ion density in the excited state and the total Ho^{3+} -ion density, respectively. The spectra are shown in Fig. 2. As can be seen, an inversion of more than 10 % is needed to reach gain in $\text{Ho}:\text{Lu}_2\text{O}_3$. For inversion levels of around 13 % the highest gain is found at 2134 nm while for increasing inversions a gain peak at 2124 nm comes up, which remains the highest peak even for very high inversion levels. This makes $\text{Ho}:\text{Lu}_2\text{O}_3$ very suitable for long wavelength ($> 2.1 \mu\text{m}$) laser operation in the Q-switched regime, which commonly requires high inversion levels. A widely used material for this is $\text{Ho}:\text{YAG}$, which however suffers from a decrease of the wavelength with maximum gain from 2129 nm (low inversions) to 2090 nm (high inversions) [8].

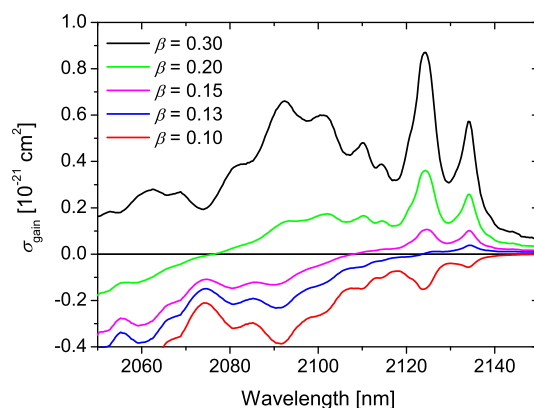


Fig. 2. Gain spectrum of $\text{Ho}:\text{Lu}_2\text{O}_3$ for different inversion levels β . For inversion levels around 13 % maximum gain can be found around 2134 nm, for high inversion levels the gain peak is located at 2124 nm.

Fluorescence Lifetime

For measuring the fluorescence lifetime of the $^5\text{I}_7$ manifold the crystal was excited by an OPO into the $^5\text{I}_6$ manifold at a wavelength of 1130 nm. The pulse length of the OPO pulses was 10 ns and therefore much shorter than the lifetime of the energy level that was to be measured. The fluorescence dynamics of the $^5\text{I}_6$ - and the $^5\text{I}_7$ -manifolds were selected with a 0.5 m monochromator and detected with an InGaAs diode. The lifetime of the $^5\text{I}_6$ -manifold was measured at around $1.2 \mu\text{m}$ to be $580 \mu\text{s}$ which is about a factor of 20 shorter than the lifetime of the $^5\text{I}_7$ -manifold, which was detected at a $\sim 50 \text{ nm}$ broad spectral region centered at 2020 nm. For assuring a neglectable impact of the decay time of the $^5\text{I}_6$ -manifold, the lifetime of the $^5\text{I}_7$ -manifold was derived from the part of the decay curve starting at 5 ms after the excitation. A fluorescence lifetime of 10 ms could be determined. This is shorter than the radiative lifetime of 14.9 ms determined by Galceran et al. from the absorption spectrum [15]. As this absorption spectrum differs from the absorption spectrum we have measured, the deviation is not surprising. With the here presented absorption spectrum a radiative lifetime of $\sim 12 \text{ ms}$ can be estimated using the same formula. The deviation to the measured fluorescence lifetime presumably occurs due to assumptions made for the estimation, as e.g. an averaged wavelength. In general no impact of non-radiative processes is expected, because > 7 phonons are needed for the transition $^5\text{I}_7 \rightarrow ^5\text{I}_8$.

4. Diode Pumped Laser Experiments

For the diode pumped laser experiments a GaSb-based laser diode stack served as the pump source. It was not designed for the experiments presented here but for the Ho:YAG experiments described in [8].

The laser diode stack consisted of ten linear bars and delivered a pump power of up to 150 W. While the central wavelength of the diode spectrum shifted from 1890 nm at threshold to 1935 nm at maximum power its spectral bandwidth (FWHM) increased from 10 nm to 30 nm (see Fig. 3).

As can be seen from Fig. 4, the pump light was focused onto a Ho(0.3%):Lu₂O₃ laser rod using an anti-reflective (AR) coated multi-lens focusing optic with $f_{\text{tot}} = 20$ mm, creating a pump spot diameter of ~ 2 mm. The laser rod was 2.5 mm in diameter and 20 mm in length. It was barrel polished to assure guiding of the pump light. Both facets were AR coated for pump and laser wavelength and it was water cooled to 18 °C. The resonator was formed by two plane mirrors, with the incoupling mirror placed as close to the laser rod as possible and the output coupling mirror 15 mm behind the crystal's rear facet, leading to a resonator length of 37 mm. The resonator was stabilized by the thermal lens inside the crystal. Between the laser rod and the output coupling mirror a water cooled pinhole (diameter = 3 mm) was placed which protected the mirror mount from heating up strongly, as it otherwise would have been irradiated by the non-absorbed pump light.

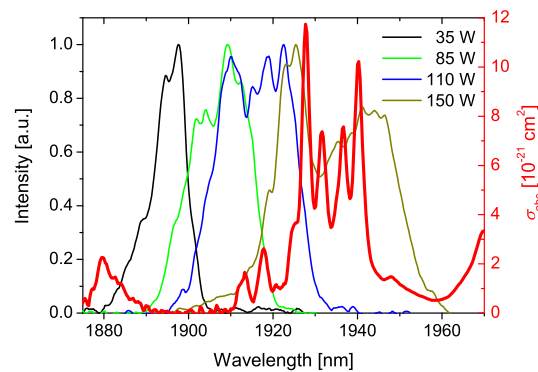


Fig. 3. Absorption spectrum of Ho:Lu₂O₃ (red, thick) and emission spectra of the laser diode for different pump powers.

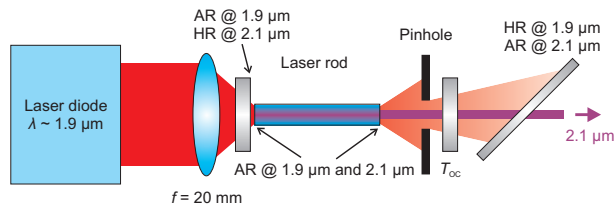


Fig. 4. Resonator setup for the diode pumped laser experiments. The water cooled pinhole prevents the mirror mount from heating up strongly.

In Fig. 3 the Ho:Lu₂O₃ absorption spectrum and the diode spectra for different pump powers can be seen. It is evident that the overlap changes for different pump powers. For calculating the absorption efficiency, the Lambert-Beer law was applied for every wavelength and the transmitted spectrum was determined theoretically. Saturation effects were not taken into account.

By comparing the area of the input and the output spectrum the fraction of absorbed power was determined. The results of this calculation are shown in black squares in Fig. 5. It can be seen that with the described pump diode moderate absorption efficiencies can only be expected at high pump powers.

For another estimation of the absorption efficiency the transmitted pump power was measured with removed output coupler for different pump power levels without lasing. The transmission is shown in blue circles in Fig. 5. For the regions of a small overlap of the absorption and the diode spectra a transmission of nearly 100 % is found. This indicates very small incoupling and guiding losses.

When comparing the calculated absorption and the measured transmission at high pump powers, a strong deviation can be seen. While theoretically a transmission of less than 60 % is expected, due to strong bleaching effects a transmission of more than 80 % is measured.

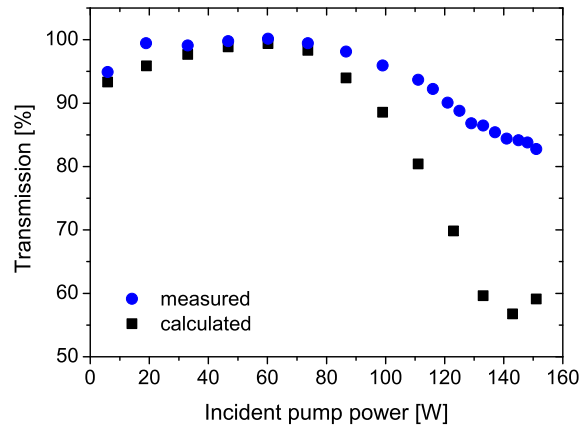


Fig. 5. Measured (blue circles) and calculated (black squares) transmission of the Ho:Lu₂O₃ rod.

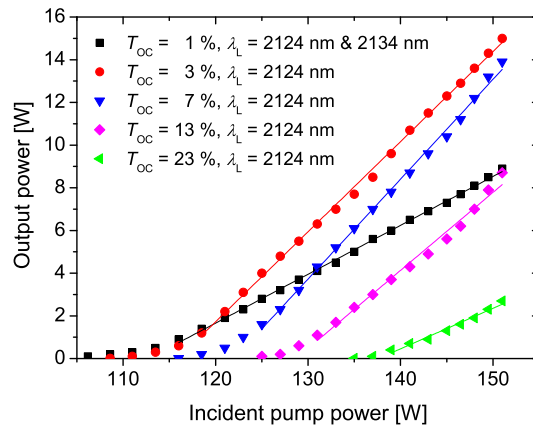


Fig. 6. Input output curves of the diode pumped Ho:Lu₂O₃ laser.

For the laser experiments output coupling transmissions T_{OC} between 1 % and 23 % were chosen. The laser characteristics versus the incident pump power are shown in Fig. 6. At a maximum incident pump power of 150 W a maximum output power of 15 W was obtained

with $T_{OC} = 3\%$. One should, however, note the very high laser thresholds of about 110 W caused by the strong shift of the diode emission with increasing output power, resulting in an overlap with the Ho-absorption only at power levels > 100 W. With respect to the measured single pass absorbed power the threshold pump powers were between 5.8 W ($T_{OC} = 1\%$) and 19 W ($T_{OC} = 23\%$). Due to the wavelength shift it is not trivial to state the absorbed pump power during laser operation. However, from Fig. 5 one can estimate the fraction of absorbed pump power to be between 40 % (calculated, neglecting thermal and bleaching effects) and 17 % (measured without lasing, thus overestimating thermal and bleaching effects), leading to an optical-to-optical efficiency with respect to the absorbed pump power between 25 % and 59 %. Considering the strong deviation between calculated and measured absorption already at the threshold pump power levels apparent in Fig. 5, one can conclude that bleaching effects are strong. Consequently, the real optical-to-optical efficiency should be in the upper range of the estimated span. Using similar assumptions, the slope efficiency with respect to the absorbed pump power can be estimated to be higher than 50 %.

Due to the very broad and strongly shifting diode spectra, calculations of saturation effects would be very speculative. We therefore refrain from it here and will address this issue with further work which will be published in the future.

The laser wavelength was 2124 nm for all output coupling rates exceeding 1 %. At $T_{OC} = 1\%$ the laser emitted at 2124 nm and 2134 nm simultaneously, with a higher intensity of the 2134 nm transition, see Fig. 7.

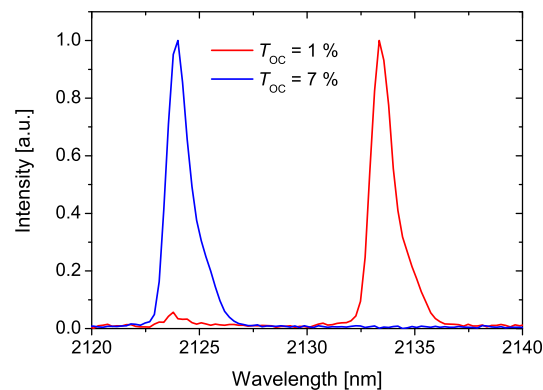


Fig. 7. Spectra of the Ho:Lu₂O₃ laser for output coupling transmissions of 1 % and 7 %.

5. Fiber Laser Pumped Laser Experiments

For improving the absorption efficiency, we have set up a grating-stabilized fiber-based master oscillator power amplifier (MOPA) system. A schematic of the setup is shown in Fig. 8. As a master oscillator a 2 m long thulium doped single mode fiber with a 10 μm core and 125 μm cladding diameter was used ($\text{NA} = 0.19$). An undoped fiber with a highly reflective fiber Bragg grating (FBG) at 1940 nm was spliced to this fiber. The grating was inscribed into the fiber with a femtosecond laser at the IPHT in Jena, Germany. The 0.5 nm broad (FWHM) 500 mW output of this fiber laser was amplified to a power of up to 17 W in a 2.2 m long thulium doped fiber (55 $\mu\text{m}/500 \mu\text{m}$, $\text{NA} = 0.22$).

The collimated output of the amplifier was focused onto the Ho:Lu₂O₃ rod described in the previous section with an $f = 80$ mm lens. For protecting the fiber from damage, an undoped fiber had to be spliced to the pumped end of the amplifying fiber. At the splice some of the 1.94 μm

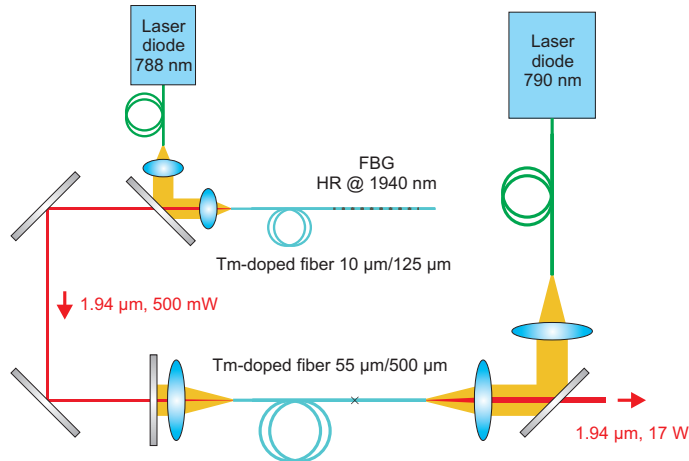


Fig. 8. Setup of the fiber based master oscillator power amplifier system.

light coupled into the cladding of the fiber. Therefore not all of the pump light was found in the $\sim 200 \mu\text{m}$ pump mode diameter but also in an area with $\sim 2 \text{ mm}$ in diameter around the pump channel. For the laser experiments this led to a decrease of the overlap with the laser mode.

The resonator was formed by a plane incoupling mirror which was AR coated for the pump and HR coated for the laser wavelength, a plane folding mirror and a spherical output coupler with $r = 200 \text{ mm}$, as shown in Fig. 9. The folding mirror ($R = 2\%$ at 1940 nm and 45°) was used to reduce the back reflection of pump light to the fiber amplifier, since no optical diode was placed between the fiber amplifier and the laser resonator. The incoupling mirror was placed as close to the laser rod as possible while the distances from the folding mirror to the rod's rear facet and the output coupler were 20 mm each. This leads to a diameter of the TEM_{00} beam inside the crystal of $\sim 440 \mu\text{m}$, which is larger than the inner part of the pump channel but smaller than the outer part. A multimode output of the laser is assumed. The cavity was stable for thermal lenses with focal lengths down to 47 mm .

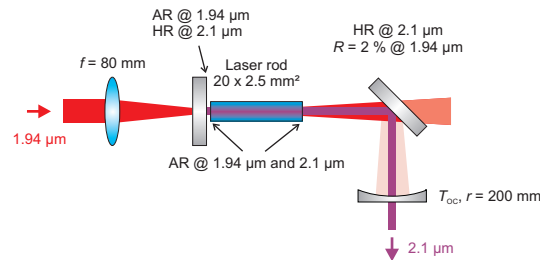


Fig. 9. Resonator setup for the fiber laser pumped laser experiments.

With the narrow linewidth pump source a single pass absorption of up to 70% could be achieved in non-lasing conditions. A strong bleaching of the absorption was observed for increasing pump powers. The absorbed pump power in lasing conditions could not be determined via measuring the transmitted pump power, because the folding mirror was small and the transmitted pump light at least partially irradiated the mirror mount. For the calculation of the absorbed pump power the absorption efficiency at threshold was determined and for higher pump powers the same absorption efficiency was assumed.

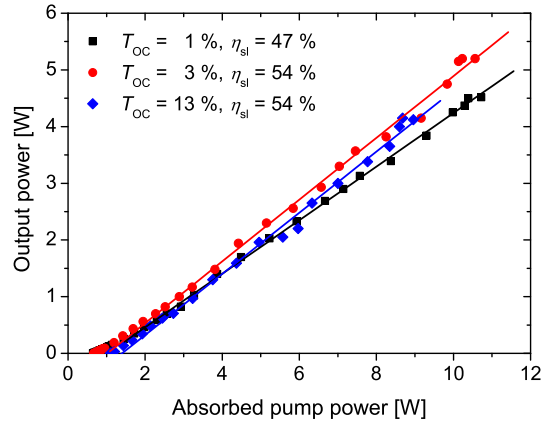


Fig. 10. Input output curves of the fiber laser pumped Ho:Lu₂O₃ laser for different output coupling transmissions.

The input output curves of the Ho:Lu₂O₃ laser are shown in Fig. 10. For 1% of output coupling the threshold pump power was as low as 650 mW. The maximum achieved output power was 5.2 W at $T_{OC} = 3\%$ while the slope efficiencies were between 47% and 54% for output coupling rates between 1% and 13%. The laser was oscillating at a wavelength of 2124 nm for all output coupling rates except for the $T_{OC} = 1\%$ mirror. In this case the laser oscillated at 2124 nm and 2134 nm simultaneously, as in the diode pumped setup. At high pump powers the laser showed an unstable behavior which was due to the imperfect suppression of back reflections of the pump light into the fiber amplifier. Therefore, for pump powers of more than 12 W (~ 8 W of absorbed power) additional wavelengths could be observed in the pump light spectrum.

6. Conclusion

We achieved the first laser operation of holmium-doped Lu₂O₃. Two different pump setups were applied for room temperature cw laser operation. In a diode pumped setup output powers of up to 15 W were obtained at a wavelength of 2124 nm. Due to a strong shift of the pump diode spectrum, laser operation could be obtained for high pump powers only. The optical-to-optical efficiency was estimated to be about 50%. Using a self-built fiber laser as the pump source, the maximum output power was 5.2 W and the maximum slope efficiency with respect to the absorbed power was 54%. Furthermore, the absorption, emission, and gain spectra of Ho:Lu₂O₃ were measured as well as the lifetimes of the ⁵I₆- and the ⁵I₇-manifolds. The crystal shows favorable properties for long wavelength laser operation above 2.1 μ m. Due to its high thermal conductivity, long lifetime, and long wavelength gain peak, Ho:Lu₂O₃ is a promising candidate as a high-power Q-switched pump source for the excitation of OPOs based on ZGP for the conversion into the mid-infrared.